MICROSTRUCTURE AND PROPERTIES OF CAST IRON AFTER LASER SURFACE HARDENING

Stanislav Němeček[1,*]

[1] MATEX PM s.r.o., Morseova 5, 301 00 Plzeň, Czech Republic

[*] corresponding author: e-mail: nemecek@matexpm.com

Resume

Laser surface hardening of cast iron is not trivial due to the material's heterogeneity and coarse-grained microstructure, particularly in massive castings. Despite that, hardening of heavy moulds for automotive industry is in high demand. The present paper summarises the findings collected over several years of study of materials structure and surface properties. Phase transformations in the vicinity of graphite are described using examples from production of body parts in automotive industry. The description relates to formation of martensite and carbide-based phases, which leads to hardness values above 65 HRC and to excellent abrasion resistance.

Available online: http://fstroj.uniza.sk/journal-mi/PDF/2013/20-2013.pdf

Article info

Article history:
Received 10 December 2012
Accepted 8 September 2013
Online 22 December 2013

Keywords:
Laser;
Surface;
Hardening;
Cast iron;
Microstructure..

ISSN 1335-0803 (print version)
ISSN 1338-6174 (online version)

1. Introduction

In a number of applications, cast iron is an irreplaceable material owing to its affordability, favourable casting properties and good machinability. Sheet forming dies for automotive industry may serve as a good example in this context. The car body consists of about 300 components, which represent a demand for about 750 pairs of press dies (progressive dies, punching and trimming dies). Car manufacturers launch about 120 new car models every year. Based on that number, the cost estimate for die making is 12 billion euro every year.

In terms of mechanical properties, cast iron – much like steel – offers a wide range of strength levels combined with good toughness and shock and vibration damping ability. Sliding properties of cast iron represent highly sought-after qualities. The wear resistance of cast iron surface can be further enhanced by surface hardening [1]. Surface hardening, regardless of the method (laser or induction), substantially improves the material's contact fatigue resistance [2] and practically doubles its wear resistance [3].

Laser hardening [4-7] is often doubted for creating overlap zones between hardening passes [8], equal to conventional heat-affected zones. This paper explores effects of these weak spots, in which the material's properties are expected to be impaired.

2. Results

In an experiment with the GG25 (EN-GJL-250**)** cast iron (chemical composition 3,1 % C, 1,47 % Si, 0,98 % Mn), the general wear resistance of laser-hardened surface was explored, as well as the wear resistance of heat-affected zones between adjacent hardening passes (believed to be the weak spots of large laser-hardened surfaces). Initial microstructure was fully pearlitic with globular graphite and hardness about 250 HV. Three plates with dimensions of 200 x150 x70 mm were hardened using three different schedules. Hardening was done using high power direct diode laser mounted on Kuka KR16 robotic system, including on line surface temperature control by 2 canal pyrometer. In each of plate, 8 passes (of 23 mm width) were made with 5 mm overlap between adjacent passes, as shown in Fig. 1. Specimens 1 and 2 were hardened at equal temperatures but the speed was three times higher in specimen 1 than in specimen 2. Specimen 3 was hardened at a speed equal to that used for specimen 1. However, its hardening temperature was 80 °C higher. Metallography was performed on Nikon light microscope with LIM analyzing software after Nital etching.

Laser-hardened cast iron with pearlite matrix, whether grey or ductile (Fig. 2a, b), typically shows hardness of 800 – 900 HV (i.e. 64 – 67 HRC). These values are the result of several hundred tests conducted during production over a period of 4 years in Matex PM company. In some cases, however, one can find lower hardness values, associated with the presence of retained austenite, as shown in Figs. 2 – 3. The hardening temperature plays a very significant role in this process. Optimum conditions promote formation of fine martensite in the vicinity of graphite particles free from retained austenite. Higher temperatures cause graphite to dissolve and lead to the supersaturation of adjacent locations with carbon. Besides the proportion of austenite, the size of martensite plates grows as well in these cases (Fig. 3). However, as the diffusion equation states, the carbon diffusion path increases with the square root of the product of time and the diffusion coefficient. Consequently, one cannot expect the same microstructure across the hardening depth, see Fig. 4. The typical hardening depth is approximately 1 mm.

The heat supplied by the laser beam promotes austenitisation of the pearlite matrix and then causes carbon to diffuse from graphite to austenite which becomes supersaturated with carbon. An appropriate combination of temperature and rate of travel of the laser beam provides an optimum microstructure of martensite and graphite (the latter provides cast iron with its expected good friction properties). Specific heat capacity of graphite exceeds that of austenite. As a result, heat accumulates in graphite particles, causing the surrounding austenite to overheat and partially melt [9, 10]. Graphite particles are then embedded in ledeburite envelopes. Where small globules were present or long heating times were used, the entire graphite globules transform into ledeburite, as shown in Fig. 3, right. This results in considerable microhardness fluctuation in specimens and leads to an overall decrease in hardness due to the presence of retained austenite.

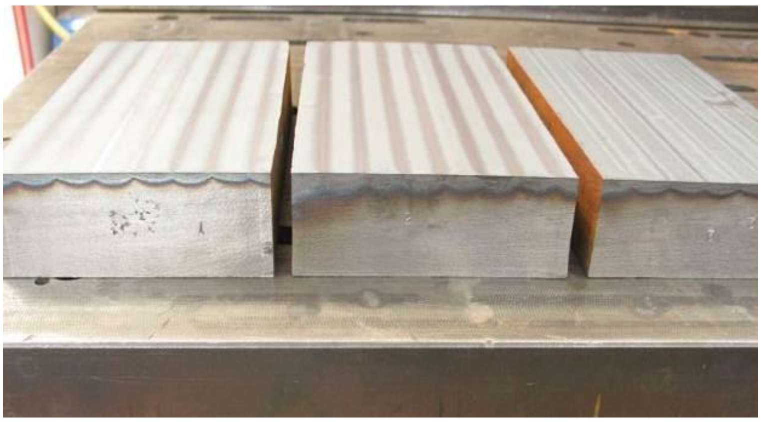

Fig.1. Specimens used in the study after laser surface hardening.
(full colour version available online)

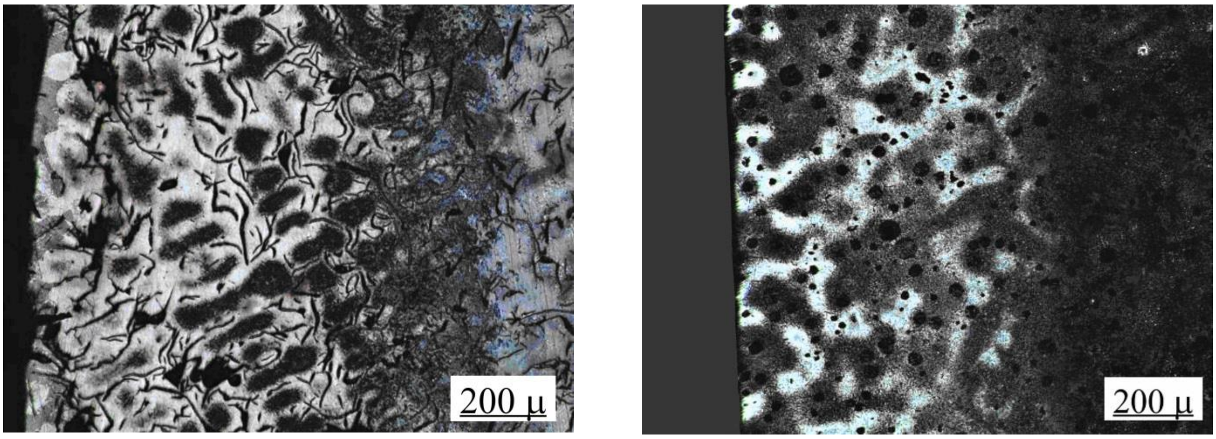

a) b)

Fig. 2. The vicinity of graphite particles is supersaturated with carbon and primary dendrite arms consist of martensite in both grey cast iron (a) and ductile cast iron (b).

(full colour version available online)

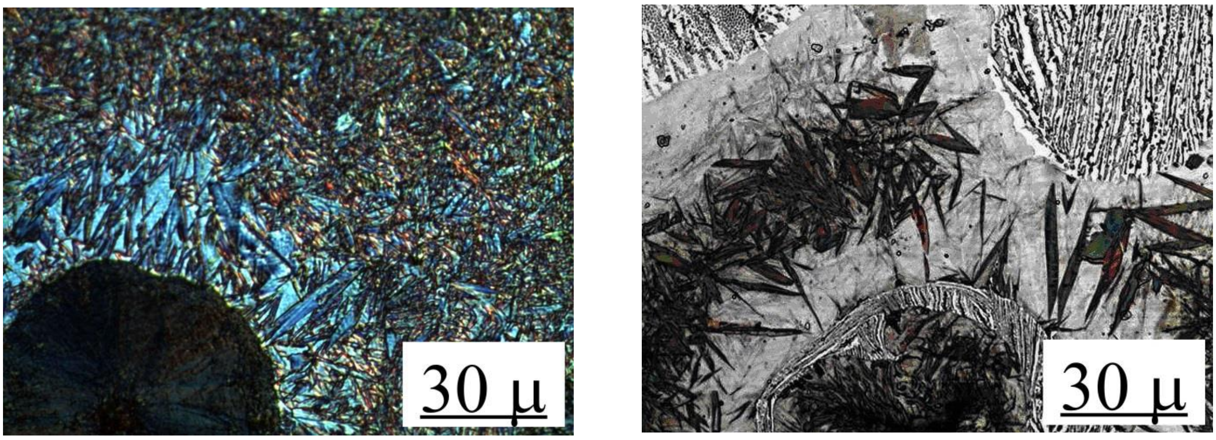

a) b)

Fig. 3. Detailed views of graphite particles and their vicinity: upon correct hardening (a), the graphite particle is surrounded by minimum amount of retained austenite and by fine martensite (the size of martensite plates is below 10 µm!); overheating causes graphite to transform into ledeburite (b) - typically for areas near the hardened surface.

(full colour version available online)

Hardness was measured on metallographic cross section perpendicularly from surface to matrix with 0.3 kg loading Vickers hardness indentor. The sub-surface hardness of specimen 1 is 700 HV; its hardness decreases linearly up to the depth of 1 mm, Fig. 4. In this case, hardness fluctuates due to the effects of heat (as in annealing). Equally, the hardness in specimens 2 and 3 decreases down to the depth of 1 mm beneath the original surface. However, their maximum hardness value is slightly higher: approx. 850 HV. The hardening depth in specimen 2 is 1.5 mm. In specimen 3, the hardening depth is 1.2 mm. The programs used for specimens 2 and 3 used lower heating rate and higher hardening temperature, respectively, than that for specimen 1. These changes improved the austenitizing process, made the carbon distribution more uniform and promoted dissolution of carbides. This is evidenced by the resulting microstructure, which exhibits smaller amount of retained austenite (which reduces the hardness of hardened surface) than in specimen 1. The material's wear resistance was explored using pin-on-disc test. The test consists in applying a load on a rotating flat specimen through a ball indenter. The indenter is pressed against the specimen using a prescribed force (exerted by a weight).

(a) Specimen 1

b) Specimen 2

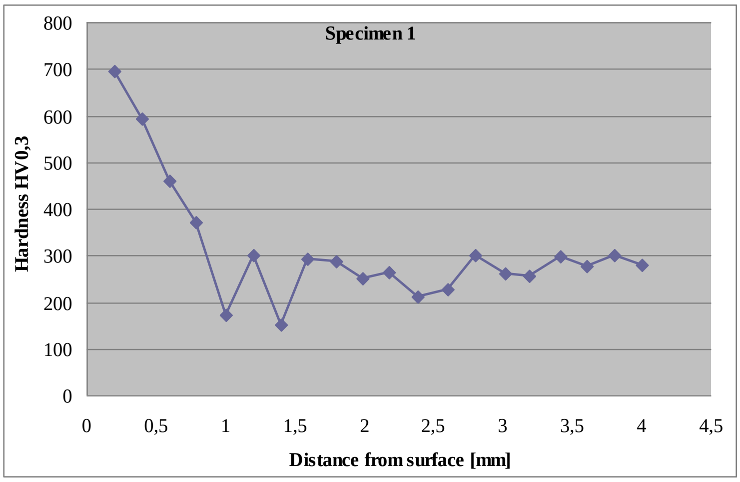

Fig. 4. Variation in microhardness of grey cast iron: the amount of austenite and the size of martensite plates decrease with increasing depth below surface: (a) lower hardening temperature - specimen 1, (b) higher hardening temperature – specimen 2.

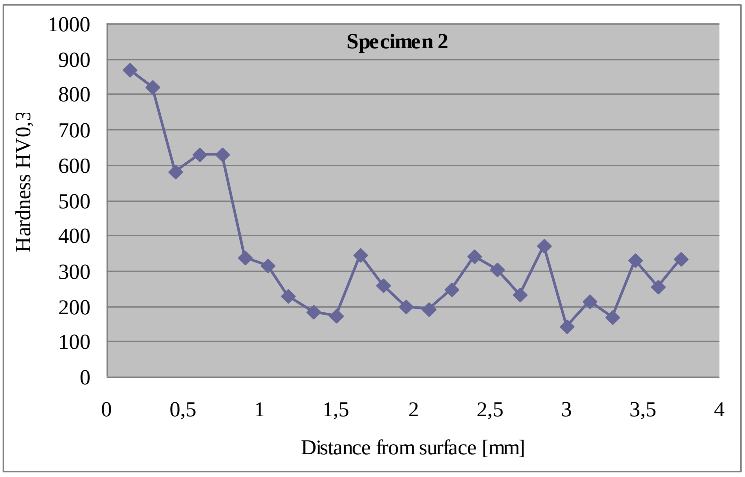

continue of Fig. 4. Variation in microhardness of grey cast iron: the amount of austenite and the size of martensite plates decrease with increasing depth below surface: (a) lower hardening temperature - specimen 1, (b) higher hardening temperature – specimen 2.

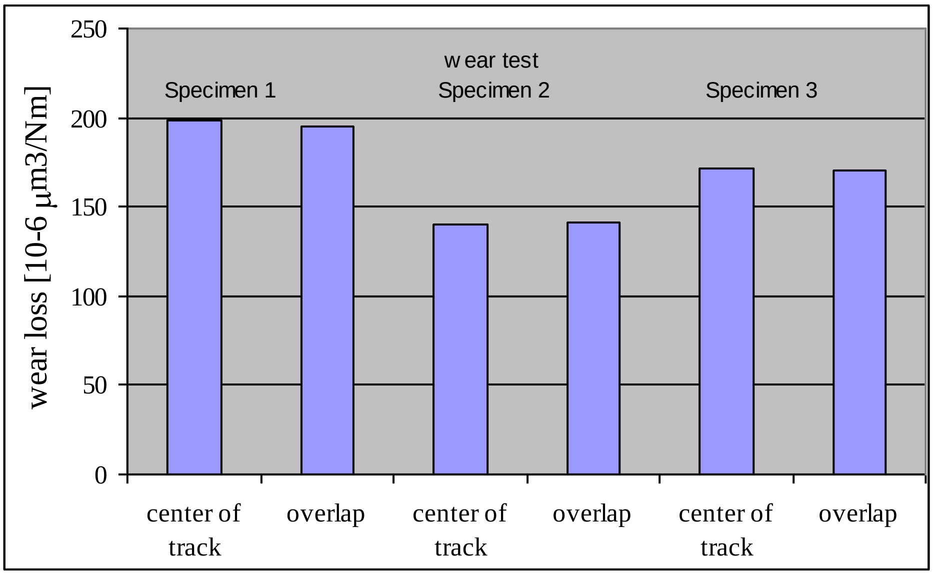

Fig. 5. Pin-on-disc tests of the centre of the hardening pass and the hardening pass overlap zone.

Table 1

Data from tribological tests – worn volume and wear loss

specimen	place	Worn volume [10^6 µm^3]	Wear loss [10^{-6} µm^3/Nm]
plate 1	center of track	186807	198
	overlap	184319	195,6
plate 2	center of track	132560	140,6
	overlap	132774	140,9
plate 3	center of track	161827	171,7
	overlap	160327	170,1

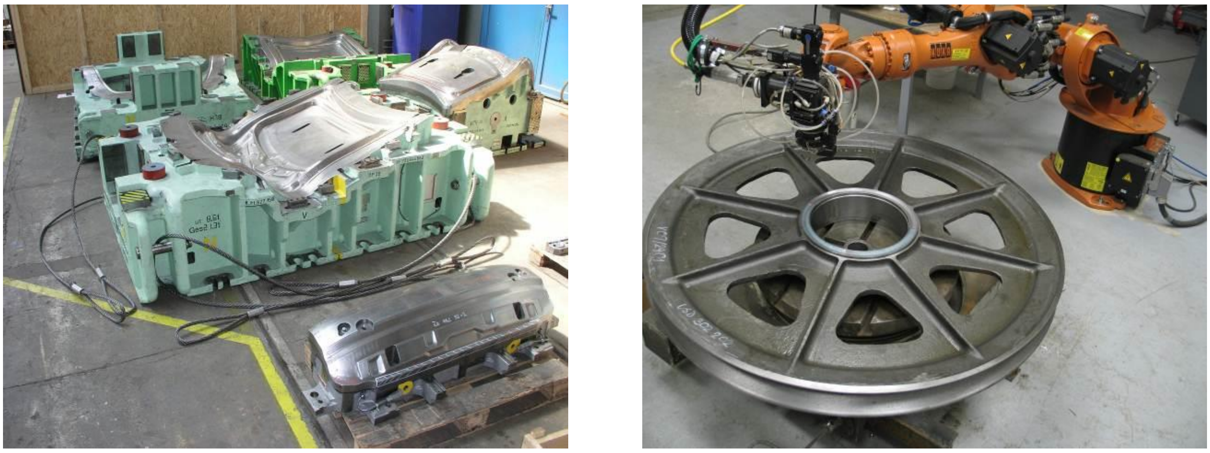

a) *b)*

Fig. 6. Laser-hardened cast iron dies, pulleys and cable wheels
(full colour version available online)

The highest wear resistance was found in specimen 2, which also exhibited the highest sub-surface microhardness of all specimens. The lowest wear resistance and hardness were found in specimen 1. No difference was found between the wear of the centre of the hardening pass and the overlap zone. The two leftmost bars in the graph in Fig. 5 represent the amount of wear of specimen 1 upon the pin-on-disc test. The left one of the pair pertains to the centre of the hardening pass, whereas the right one relates to the heat-affected zone. Equal heights of both bars signify equal amounts of wear. The overlap of hardening passes therefore does not pose any greater risk of wear than other locations. The additional two pairs of bars denote specimens 2 and 3. In these specimens too, no difference between the centre of the hardening pass and the overlap zone was found.

3. Conclusion

Poor thermal conductivity of cast iron leads to its low hardening depths: typically less than 1 mm. Hardness fluctuation may reflect the coarse-grained initial microstructure of castings but more likely causes can be found in the transformation of graphite into ledeburite and in the presence of retained austenite. Despite that, martensite formed upon laser hardening exhibits fine laths and plates. Tempered zones of overlap of hardening passes exhibit approx. 5 HRC lower hardness than the centres of hardening passes. Yet, pin-on-disc testing of wear behaviour revealed that wear in these locations is not greater than in other parts of the hardened surface. In tens of projects involving hardening of steels (including carburised steels) and cast irons with high carbon levels in the matrix, no surface cracks were found in any of the parts. There is the only risk resulting from the use of excessively high temperature: evaporation of graphite from the surface (which, however, commonly takes place during all other surface hardening processes) and a decline in hardness due to formation of retained austenite. With this being said, laser hardening remains the method of choice among other surface hardening processes. Laser hardening of cast iron has become an accepted and ever more widespread technique for strengthening the surface of cast iron, as illustrated in Fig. 6.

Acknowledgment

This paper presents results of the project no. TIP FR-TI3/814: "Laser surface processing optimization of engineering components for their quality properties enhancement" funded from the Ministry of Industry of the Czech Republic.

References

[1] A. H. Backar: Production Engineering and Design for Development, Cairo 2006.

[2] T. Zengyi, L. Jiaming: Acta Metall. Sin. 3 (1990) 188-193.

[3] J. - H. Hwang et al.: J. Mater. Eng. Perform 11 (3) (2002) 294-300.

[4] M. W. Steen, J. Mazumder: Laser Mat. Process. Springer, New York 2003.

[5] S. Němeček: Adv. Mat. Res. III, (2013) 92-97.

[6] T. Mužík, S. Němeček, K. Štěpán: In: 9.Workshop Industrielle Anwendungen von Hochleistungs-Diodenlasern, Fraunhofer IWS, Dresden 2012.

[7] J. Grum: J. Achievements in Mat. Manufacturing Eng. 24 (2007) 17-25.

[8] R. Rowshan: Process Control During Laser Transformation Hardening. PhD thesis, University of Miskolc, Hungary 2007.

[9] J. Grum, R. Šterm: Mater. Charact. 37 (1996) 81-88.

[10] Y. Chen, C.H. Gan, L.X. Wang, G. Yu, A. Kaplan: Appl. Surf. Sci. 245 (2005) 316-321.